

Journal of Materials Chemistry B

Accepted Manuscript



This is an *Accepted Manuscript*, which has been through the Royal Society of Chemistry peer review process and has been accepted for publication.

Accepted Manuscripts are published online shortly after acceptance, before technical editing, formatting and proof reading. Using this free service, authors can make their results available to the community, in citable form, before we publish the edited article. We will replace this *Accepted Manuscript* with the edited and formatted *Advance Article* as soon as it is available.

You can find more information about *Accepted Manuscripts* in the [Information for Authors](#).

Please note that technical editing may introduce minor changes to the text and/or graphics, which may alter content. The journal's standard [Terms & Conditions](#) and the [Ethical guidelines](#) still apply. In no event shall the Royal Society of Chemistry be held responsible for any errors or omissions in this *Accepted Manuscript* or any consequences arising from the use of any information it contains.



SCHOLARONE™
Manuscripts

Biodegradable Glycopolymer-*b*-Poly(ϵ -caprolactone) Block Copolymer Micelles: Versatile Construction, Tailored Lactose Functionality, and Hepatoma-Targeted Drug Delivery

Wei Chen^{1,2}, Fenghua Meng¹, Ru Cheng¹, Chao Deng¹, Jan Feijen^{1,2,*}, and Zhiyuan Zhong^{1,*}

¹ Biomedical Polymers Laboratory, and Jiangsu Key Laboratory of Advanced Functional Polymer Design and Application, Department of Polymer Science and Engineering, College of Chemistry, Chemical Engineering and Materials Science, Soochow University, Suzhou, 215123, P. R. China.

² Department of Polymer Chemistry and Biomaterials, Faculty of Science and Technology, MIRA Institute for Biomedical Technology and Technical Medicine, University of Twente, P.O. Box 217, 7500 AE Enschede, The Netherlands.

*Corresponding authors. Tel/fax: +86-512-65880098; E-mail: j.feijen@utwente.nl;

zyzhong@suda.edu.cn

Abstract

Glycopolymer-*b*-poly(ϵ -caprolactone) (GP-PCL) block copolymer micelles ('glycomicelles') with tailored lactose functionalities were developed and investigated for hepatoma-targeted doxorubicin (DOX) delivery. Amphiphilic GP-PCL copolymers were readily prepared with controlled lactobionic acid (LBA) functionalities of 20%, 40%, 80%, and 100% (denoted as GP20-PCL, GP40-PCL, GP80-PCL, and GP100-PCL, respectively) through

post-polymerization modification of poly(acryloyl cyclic carbonate)-*b*-poly(ϵ -caprolactone) (PAC-*b*-PCL, 11.6-6.4 kg/mol) block copolymer with thiolated LBA (LBA-SH) and 2-(2-methoxyethoxy)ethanethiol ((EO)₂-SH) via Michael-type addition reaction. These self-assembled glycomicelles had mean hydrodynamic diameters ranging from 31.9 to 76.8 nm depending on LBA densities, and exhibited high DOX loading efficiencies of 83.0-89.2%. *In vitro* release studies showed that the DOX release rate depended on pH and LBA content. Flow cytometric analyses revealed that asialoglycoprotein receptor (ASGP-R) over-expressed HepG2 liver cancer cells following 4 h treatment with DOX-loaded glycomicelles had a 6.6-17.1 fold higher DOX level, depending on LBA densities, as compared to those treated with the corresponding DOX-loaded non-glycomicelles (100% substitution with (EO)₂-SH) under otherwise the same conditions. MTT assays demonstrated that DOX-loaded GP20-PCL, GP40-PCL, GP80-PCL and GP100-PCL micelles had much lower half maximal inhibitory concentration (IC₅₀) values of 2.05, 0.75, 0.45 and 0.43 μ g DOX equiv./mL, respectively, in HepG2 cells than DOX-loaded non-glycomicelles (IC₅₀: 6.55 μ g/mL DOX equiv./mL). Competitive inhibition experiments showed that after the incubation with DOX-loaded glycomicelles for 4 h, more efficient killing activity against free HepG2 cells (- LBA) was observed, as compared to that against LBA-blocked HepG2 cells (+ LBA) after a subsequent 72 h incubation. Glycomicelles with tailored LBA functionalities, high drug loading capacity, and high uptake by ASGP-R positive cells are promising for liver cancer chemotherapy.

Keywords: Glycopolymer, biodegradable micelles, Michael addition, liver cancer, drug delivery.

Introduction

Biodegradable micelles based on polylactide (PLA), poly(ϵ -caprolactone) (PCL), and poly(lactide-*co*-glycolide) (PLGA) have appeared as one of the most promising nanosystems for targeted cancer chemotherapy.¹⁻⁷ In particular, they are suited for delivery of hydrophobic anti-cancer drugs such as paclitaxel (PTX) and doxorubicin (DOX), which can be efficiently loaded into the core of micelles. Various *in vivo* studies demonstrated that they could prolong drug circulation time, passively target to the tumor tissues via the enhanced permeability and retention (EPR) effect, decrease side effects, and improve drug tolerance.^{8,9} It should be noted, however, that the therapeutic outcome of current micellar drugs is not optimal partially due to inferior tumor cell uptake as a result of PEG shielding.^{10,11} Surface decoration of micellar nanosystems with specific ligands such as proteins, peptides, folic acid (FA), and saccharide/poly saccharide, have shown to significantly improve retention and accumulation of nanoparticles in the tumor vasculature as well as selective and efficient internalization by target tumor cells.¹²⁻¹⁶

It is generally accepted that the presence of multiple ligands on the surface of nano-sized drug formulations can improve the cell targeting as well as the therapeutic efficacy.¹⁷ Lee et al. firstly reported that saccharide assemblies (glyco-clusters) could strongly bind to proteins, and that the interactions between saccharides and proteins and/or cells were much affected by the saccharide density.¹⁸ This multivalent interaction was called “glycoside cluster effect”. Various “glyco-clusters” have been reported, such as glycol-modified cyclodextrins,¹⁹ glycopeptides^{20,21}, and polymers with pendant saccharides (glycopolymers).^{22,23} Well-defined synthetic glycopolymers have recently received much attention in sugar-related drug discovery, molecular diagnosis, and targeted drug/gene delivery, since these glycopolymers have the appropriate physical properties and material workability to improve the binding affinity for specific proteins.²⁴⁻²⁸

In recent years, it has been demonstrated that micellar nanoparticles decorated with β -D-galactose, *N*-acetylgalactosamine, and lactose ligands can be used for the targeting of hepatoma cells that are over-expressed with asialoglycoprotein receptors (ASGP-R).²⁹ Interestingly, lactobionic acid (LBA), containing the lactose residue, also works as an efficient ligand for recognition of ASGPR, and therefore, LBA-decorated drug delivery systems can successfully target hepatocytes.²⁹⁻³¹ To result in more efficient cellular uptake and higher drug efficacy, a number of galactosyl or its analogues decorated glycopolymer architectures including linear polymers,³²⁻³⁷ dendrimers,³⁸⁻⁴⁰ and micellar nanoparticles,⁴¹⁻⁴⁴ have been developed for enhanced hepatoma-targeted drug delivery. For example, Yang *et al.* prepared biodegradable amphiphilic glycopolymer-PTMC block copolymers by sequential ring-opening copolymerization of protected sugar-containing carbonate monomers and TMC, followed by deprotection.⁴⁵ They found that these glycomicelles exhibited significant cellular uptake and anti-tumor efficacy using ASGP-R positive HepG2 cells. Recently, we reported PCL-*graft*-SS-lactobionic acid (PCL-g-SS-LBA) glyco-nanoparticles (SS-GNs) with sheddable saccharide shells as a unique and potent platform for hepatoma-targeted delivery of DOX. It was demonstrated that SS-GNs could be efficiently taken up by HepG2 cells, and DOX was released into the nuclei of cells following only 4 h incubation due to the fast cleavage of S-S bonds at intracellular reductive conditions.⁴⁶

Although high ligand densities on the nanosystems might be desirable from the perspective of enhanced binding towards target cells, it should be noted that nanosystems with high densities have been associated with increased possibilities of clearance from the circulation, which would probably result in decreased accumulation of the carriers in the target tissue.¹⁵ There is little work that has been done to determine whether an optimal ligand density exists on biodegradable nanosystems for targeted drug delivery. In this study, we aimed to develop novel biodegradable glycomicelles with tailored LBA densities for active

hepatoma-targeted drug delivery (Scheme 1). Biodegradable PAC-*b*-PCL block copolymer can be readily prepared by one-pot sequential ring-opening polymerization (ROP) of acryloyl cyclic carbonate (AC) and ϵ -CL. PAC-*b*-PCL is amenable to the Michael-type addition reaction with thiolated LBA (LBA-SH) and (EO)₂-SH, which yields glycopolymer-*b*-PCL with varying LBA functionalities. Synthesis and self-assembly of biodegradable block glycopolymers, loading and *in vitro* release of DOX, as well as the uptake of DOX-loaded glycomicelles with different LBA densities using HepG2 cells and their toxicity towards these cells have been investigated.

Materials and methods

Materials

2-(2-Methoxyethoxy)ethanethiol ((EO)₂-SH, 97%, Aldrich), lactobionic acid (LBA, 97%, Acros), dithiothreitol (DTT, 99%, Merck), N-hydroxysuccinimide (NHS, 98%, J&K), 1-ethyl-3-(3-dimethylaminopropyl)carbodiimide hydrochloride (EDC, 98%, J&K), zinc bis[bis(trimethylsilyl)amide] (97%, Aldrich), triethylamine (Et₃N, 99%, Alfa Aesar), and doxorubicin hydrochloride (DOX·HCl, 99%, Beijing Zhong Shuo Pharmaceutical Technology Development Co. Ltd.) were used as received. ϵ -Caprolactone (ϵ -CL, 99%, Alfa Aesar) was dried over CaH₂ and distilled under reduced pressure prior to use. Acryloyl cyclic carbonate monomer (AC) was synthesized according to our previous report.⁴⁷ Isopropanol and dichloromethane (DCM) were dried by refluxing over CaH₂ under an argon atmosphere. Thiolated lactobionic acid (LBA-SH) with an SH-functionality of 80% was synthesized from LBA and 2-mercaptoethylamine using carbodiimide chemistry as reported in our previous report.⁴⁶

Synthesis of PAC-*b*-PCL block copolymer

The PAC-*b*-PCL block copolymer was synthesized by one-pot sequential ring-opening polymerization of AC and ϵ -CL in DCM using isopropanol as an initiator and zinc bis[bis(trimethylsilyl)amide] as a catalyst. Briefly, in a glove-box under a nitrogen atmosphere, to a stirred solution of AC (0.520 g, 2.60 mmol) in DCM (2.6 mL) was quickly added isopropanol stock solution (0.26 mL, 200 mM) and zinc bis[bis(trimethylsilyl)amide] stock solution (0.20 mL, 100 mM). The reaction vessel was sealed and the reaction mixture was magnetically stirred for 4 h at room temperature in the glove box. A sample was taken for determination of AC monomer conversion and polydispersity using ^1H NMR and GPC, respectively. Then the second monomer ϵ -CL (0.296 g, 2.60 mmol) in 2.6 mL of DCM was added. The reaction was allowed to proceed at 40 °C for another 20 h. Also, one sample was taken for determination of ϵ -CL conversion using ^1H NMR. The copolymer was isolated by precipitation into cold diethyl ether and dried *in vacuo* at room temperature. ^1H NMR (400 MHz, CDCl_3) for PAC-*b*-PCL copolymer: δ 1.06 (-C(CH₂)CH₃, PAC), 1.38 (-CH₂CH₂CH₂-, PCL), 1.65 (-CH₂CH₂CH₂-, PCL), 2.30(-C(O)CH₂-, PCL), 4.05 (-CH₂-O-C(O)-, PCL), 4.11 (-CH₂-O-C(O)-O-CH₂-, PAC), 5.85-6.43 (double bond, PAC).

Synthesis of glycopolymer-PCL copolymer (GP-PCL)

The synthesis of GP-PCL copolymers by Michael-type addition was carried out in DMSO/DMF at room temperature under a nitrogen atmosphere. GP-PCL copolymers with different amounts of LBA pending groups were synthesized by controlling the feed ratio of (EO)₂-SH and LBA-SH. As an example of the synthesis of GP20-PCL, to a solution of PAC-*b*-PCL copolymer (50 mg, 16 μmol of AC units) and LBA-SH (1.8 mg, 3.5 μmol of SH groups) in 3 mL of DMSO/DMF (v/v = 5/1) under a nitrogen atmosphere was added a

catalytic amount of Et_3N . The reaction was allowed to proceed with stirring for 8 h at room temperature. One sample was taken for determination of the functionality of the PAC segment using ^1H NMR. To the rest of the reaction solution, $(\text{EO})_2\text{-SH}$ (2.6 mg, 19 μmol of SH groups) dissolved in 0.5 mL of DMSO was added. The reaction was allowed to proceed at room temperature for another 8 h. The resulting GP-PCL copolymer was isolated by dialysis against deionized water to remove excess thiol-containing molecules with a molecular weight cut-off (MWCO) of 3500 at room temperature for 48 h, and freeze-dried.

Characterization

^1H NMR spectra were recorded on the Unity Inova 400 operating at 400 MHz. CDCl_3 and $\text{DMSO-}d_6$ were used as solvents and the chemical shifts were calibrated against residual solvent signals. The molecular weight and polydispersity of the copolymers were determined by a Waters 1515 gel permeation chromatograph (GPC) instrument equipped with two linear PLgel columns (500 Å and Mixed-C) following a guard column and a differential refractive-index detector. The measurements were performed using CHCl_3 as the eluent at a flow rate of 0.5 mL/min at 30 °C and a series of narrow polystyrene standards for the calibration of the columns.

Micelle formation and critical micelle concentration

Micelles were typically prepared under stirring by dropwise addition of 200 μL of copolymer solution in DMSO (2.0 mg/mL) to 2 mL of ultrapure water at room temperature, followed by dialysis to remove the organic solvent. The size, size distribution and surface charge of the micelles were determined by dynamic light scattering (DLS) and zeta potential measurements. Measurements were carried out at 25 °C with three independent replicates using a Zetasizer Nano-ZS from Malvern Instruments equipped with a 633 nm He-Ne laser using

back-scattering detection. The data are presented as mean value \pm standard deviation.

The critical micelle concentration (CMC) was determined using pyrene as a fluorescent probe. The concentration of functional copolymer was varied from 1.0×10^{-5} to 0.5 mg/mL and the concentration of pyrene was fixed at 1.0 μ M. Fluorescence spectra were recorded using a FLS920 fluorescence spectrometer and an excitation wavelength of 330 nm. Fluorescence emissions at 372 and 383 nm were monitored. The CMC was estimated as the cross-point when extrapolating the intensity ratio I_{372}/I_{383} at low and high concentration regions. The stability of the micelles in PB (pH 7.4, 10 mM) containing 10% (v/v) fetal bovine serum (FBS) was studied at 37 °C by monitoring the particle size change as a function of time using DLS.

Loading of DOX into micelles and *in vitro* release

DOX was loaded into micelles by dropwise addition of a mixture of 200 μ L of copolymer solution in DMSO (2.0 mg/mL) and 20 μ L of DOX solution in DMSO (5 mg/mL, theoretical drug loading content was set as 20%) to 2 mL of ultrapure water under stirring at room temperature, followed by stirring for 0.5 h and dialysis against deionized water with MWCO of 3500 at room temperature in the dark for 8 h.

The release profiles of DOX from the micelles were studied using a dialysis tube (MWCO 12 000) in PB (10 mM, pH 7.4) or acetate buffer (10 mM, pH 5.0) at 37 °C. In order to acquire sink conditions, drug release studies were performed with 0.6 mL of micelle suspension with a DLC of 5 wt.%, which were dialyzed against 20 mL of the same medium. At desired time intervals, 5.0 mL release media was taken out and replenished with an equal volume of fresh media. The amount of DOX released was determined by using fluorescence (FLS920) measurements (excitation at 480 nm). For determination of the drug loading content (DLC), DOX-loaded micellar suspensions were freeze-dried, then dissolved in DMSO and

analyzed with fluorescence spectroscopy. A calibration curve was obtained using DOX/DMSO solutions with different DOX concentrations. To determine the amount of DOX released, calibration curves were run with DOX/phosphate buffer solution (pH 7.4, 10 mM) with different DOX concentrations. The emission at 600 nm was recorded. Release experiments were conducted in triplicate. The results presented are the average data \pm standard deviation.

DLC and drug loading efficiency (DLE) were calculated according to the following formulas:

$$\text{DLC (wt.\%)} = (\text{weight of loaded drug} / \text{total weight of polymer and loaded drug}) \times 100\%$$

$$\text{DLE (\%)} = (\text{weight of loaded drug} / \text{weight of drug in feed}) \times 100\%$$

Analysis of the cellular uptake of DOX-loaded micelles by flow cytometry

HepG2 cells were seeded onto 6-well plates at 1.0×10^5 cells per well for 24 h using DMEM medium containing 10% FBS. After 24 h incubation, the medium was replaced by 0.9 mL of fresh DMEM and 0.1 mL of prescribed amounts of DOX-loaded micelles. After incubation at 37 °C for 4 h, the cells were digested by 0.25 w/v% trypsin/0.03 w/v% EDTA. The suspensions were centrifuged at 1500 rpm for 5 min at 25 °C, pelleted in eppendorf tubes, washed twice with cold PBS, and then resuspended in 500 μ L of PBS. Fluorescence histograms were recorded with a BD FACSCalibur (Beckton Dickinson) flow cytometer and analyzed using Cell Quest software. We analyzed 10 000 gated events to generate each histogram. The gate was arbitrarily set for the detection of DOX fluorescence.

MTT assays

The cytotoxicity of micelles and DOX-loaded micelles was studied by MTT assays using HepG2 and MCF-7 cells. Cells were seeded onto a 96-well plate at a density of 1×10^4 cells

per well in 100 μL of Dulbecco's Modified Eagle medium (DMEM) containing 10% FBS and incubated for 72 h (37 $^{\circ}\text{C}$, 5% CO_2). The medium was replaced by 90 μL of fresh DMEM medium containing 10% FBS and 10 μL of various concentrations of the micelle suspension samples. The cells were incubated for another 72 h, the medium was aspirated and replaced by 100 μL of fresh medium, and 10 μL of MTT solution (5 mg/mL) was added. The cells were incubated for 4 h, and then the medium was aspirated and replaced by 150 μL of DMSO to dissolve the resulting purple crystals. The optical densities at 570 nm were measured using a BioTek microplate reader. Cells cultured in DMEM medium containing 10% FBS (without exposure to micelles) were used as controls.

To evaluate whether the high drug efficacy was specifically caused by ASGP-R mediated endocytosis, HepG2 cells seeded in a 96-well plate at a density of 1×10^4 cells per well for 24 h were incubated with (+ LBA) or without (-LBA) free LBA (2 mg/mL) 4 h before the addition of DOX-loaded micelles or free DOX. The ASGP-R on the HepG2 cell surface can be blocked in DMEM medium containing free LBA. The cytotoxicity studies for DOX-loaded glycomicelles, DOX-loaded non-glycomicelles and free DOX (drug dosage of 10 $\mu\text{g}/\text{mL}$) were carried out as mentioned above.

Results and discussion

Synthesis of PAC-*b*-PCL block copolymer

PAC-*b*-PCL block copolymer was readily prepared by sequential ring-opening polymerization of AC and ϵ -CL in DCM (Scheme 2). The polymerization of AC was carried out using isopropanol as an initiator and zinc bis[bis(trimethylsilyl)amide] as a catalyst in DCM for 4 h at room temperature. This zinc-based catalyst is very efficient for ROP of lactones, lactides and cyclic carbonates, and several functional polycarbonate-based copolymers have been developed for biomedical applications using this catalyst.⁴⁸ Cell experiments or in vivo tests

using these polymers did not reveal any cytotoxicity problems. ^1H NMR showed that the AC monomer conversion was close to 100 % (Fig. S1a). Then, the second monomer, ϵ -CL, was added and the polymerization was allowed to continue for another 20 h at 40 °C. ^1H NMR showed complete ϵ -CL monomer conversion. PAC-*b*-PCL block copolymer was isolated by precipitation in diethyl ether. ^1H NMR showed signals characteristic of both AC units (δ 5.85-6.43, 4.11 and 1.06) and CL units (δ 4.05, 2.30, 1.65 and 1.38) (Fig. S1b). Importantly, signals due to acryloyl protons at δ 5.85-6.43 were maintained, indicating that AC functional groups remained intact during sequential polymerization and subsequent work-up procedures. The number-average molecular weights (M_n) of PAC and PCL segments estimated from ^1H NMR end group analysis by comparing the integrals of peaks at 1.06 (methyl protons in PAC block) and 2.30 (methylene protons next to carbonyl in PCL block) with δ 1.25 (methyl protons of isopropyl ester end group) were 11.6 kg/mol and 6.4 kg/mol, respectively, which were close to the theoretical values (PAC: 10 kg/mol, 50 monomer units; PCL: 5.7 kg/mol, 50 monomer units). Gel permeation chromatography (GPC) measurements using polystyrenes as standards showed that the PAC block had a relatively narrow PDI of 1.23, while the PAC-*b*-PCL block copolymer had a moderate PDI of 1.78 (Fig. S2), which was probably due to the reduced activity of the macro-initiator (PAC block) for the second PCL block synthesis, as well as the possibility of transesterification after long reaction times.

Synthesis of GP-PCL copolymer

The functionalization of PAC-*b*-PCL was performed in DMSO/DMF at room temperature by a sequential Michael-type addition reaction with LBA-SH and (EO) $_2$ -SH, to afford amphiphilic glycopolymer-PCL block copolymers with different LBA functionality (Scheme 2). For the 100% functionalization of PAC-*b*-PCL copolymer with LBA (denoted as GP100-PCL), excessive LBA-SH was added to react with the double bonds. ^1H NMR spectra

(Fig. 1a) displayed new signals at δ 3.2-3.7 (attributed to the LBA pendants), and 2.6-2.8 (the methylene protons derived from the Michael addition of acryloyl groups). It should be noted that 100% functionalization with LBA-SH was achieved based on the complete disappearance of peaks assignable to acryloyl groups. For the modification of PAC-*b*-PCL copolymer to polymers with LBA functionalities of 80, 40, and 20% (GP80-PCL, GP40-PCL and GP20-PCL, respectively), quantitative amounts of LBA-SH (the corresponding molar ratios of LBA-SH/AC units of 0.8, 0.4 and 0.2, respectively) were firstly added, followed by the addition of excess (EO)₂-SH to completely functionalize the residual AC groups. The amounts of LBA present in the copolymers were determined by comparing the integrals of resonances at 1.06 (methyl protons in PAC block) with those of remaining acryloyl groups of the sample solution, from which it was found that the LBA-functionality of all the copolymers was close to what was anticipated. After (EO)₂-SH addition, the rest of the double bonds were quantitatively functionalized (Fig. 1b). A copolymer modified with only (EO)₂-SH pendants was prepared as non-LBA control (denoted as P(EO)-PCL). ¹H NMR spectra also showed the successful modification (Fig. 1c). The ratio of integrals of resonances at 1.06 (methyl protons in PAC block) and 2.30 (methylene protons next to the carbonyl in the PCL block) did not change, which suggests that the block copolymers did not degrade during the modification procedures.

Formation of glycomicelles and non-glycomicelles

Micelles were prepared by the solvent exchange method. The organic solvent was easily removed by dialysis in water, and the hydrophobic PCL blocks of the amphiphilic polymers aggregated in water to facilitate the formation of micellar structures. The sizes of micelles were determined by dynamic light scattering (DLS) measurements (Table 1). Notably, these copolymers formed micelles with average sizes of 31.9-88.2 nm and low polydispersities

(PDIs) of 0.07-0.18 (Fig. 2). The micelle size decreased with increasing amounts of LBA, likely due to a higher hydrophilic/hydrophobic ratio. The critical micelle concentration (CMC) determined using pyrene as a probe showed that all copolymers had low CMCs of 3.72~1.03 mg/L, respectively (Table 1). The CMC of the copolymers decreased with increasing amounts of (EO)₂ on the micelle surface, indicating that the stability of the micelles increased with increased (EO)₂-functionalization. Zeta potential measurements showed that the completely LBA-functionalized micelles had positive surface charges (5.3 mV) in water (Table 1), which is likely due to weak protonation of lactose/galactose (pKa ≈ 12.4) on the micellar surface.⁴⁹ However, micelles, shielded with various molar percentages of oligo(EO) had close to neutral or even a negative surface charge (-0.1 ~ -16.5 mV), indicating that the surface charge of the micelles could be well regulated by varying the lactose content of the micelles.

The stability of the micelles in PB (pH 7.4, 10mM) containing 10% FBS at 37 °C was studied by monitoring the particle size in time. The stability of the micelles was confirmed by the absence of large aggregates and preservation of particle size. The size of the micelles remained unchanged for 12 h, indicating that the presence of serum did not affect the stability of the micelles.

Loading and *in vitro* release of DOX

DOX was loaded into micelles at theoretical drug loading contents (DLC) of 20 wt.%. Interestingly, the different micelles exhibited similar DOX loading levels (Table 3, DLE: 82.3~89.2%), indicating that the molecular weights and character of the hydrophilic segments had little influence on the drug loading behavior, which preferentially depended on the hydrophobic PCL core. Moreover, the size and size distribution of the micelles were not affected significantly after loading DOX. The diameters of the micelles increased somewhat compared to the blank micelles possibly because of an increase in the inner core volume after

loading DOX.⁵⁰

The *in vitro* release of DOX from the different micelles (DLC of 5 wt.%) was investigated using a dialysis tube (MWCO 12000) in PB (10 mM, pH 7.4) or acetate buffer (10 mM, pH 5.0) at 37 °C. There is no burst drug release from the micelles at both pH's. It is interesting to note that DOX release from all the micelles was faster at pH 5.0 than at pH 7.4. For example, GP80-PCL micelles, released very limited DOX (ca. 16.4%) in 12 h at a mimicking physiological pH condition, and approximate 40.3% of DOX was detected in the following 72 h; while the DOX release could reach ca. 73.1% at pH 5.0 after 72 h incubation (Fig. 3). This pH-dependent release behavior of DOX was also observed for PEG-*b*-PCL micelles, although with a much lower drug release rate (approximately 30% release in 3 d and 65% in 35 d).⁵¹ The faster release of DOX from the micelles under acidic conditions is likely due to improved water solubility of DOX following protonation. A similar DOX release behavior was also observed using our previously reported PCL-*g*-PHEMA graft copolymer micellar system.⁵² It should be further noted that the drug release rate increased with increasing LBA density, in which 80.9%, 73.1%, 57.7% and 50.8% of DOX was released in 72 h at pH 5.0 from GP100-PCL, GP80-PCL, GP40-PCL, and P(EO)-PCL micelles, respectively (Fig. 3). This is likely due to the faster diffusion rate of DOX at a mildly acidic pH from smaller micelles with more LBA decoration. Polymers functionalized with more ligands formed micelles containing less unimers (therefor smaller micelles). In these micelles DOX was probably less stabilized in the core and could be released more easily.

Targeted cellular uptake of DOX-loaded micelles

HepG2 cells are usually employed as a suitable model system for studies of liver metabolism, liver disease, and liver tumor targeted drug therapy.^{31, 35, 53-55} HepG2 cells were incubated with DOX-loaded glycomicelles with different LBA densities for a period of 4 h, and the targeting

efficiency was determined by calculating the amount of endocytic DOX in the cells which was analyzed quantitatively via flow cytometry. The contribution of DOX still present in the core of the micelles to the fluorescence of the cells will be negligible due to self-quenching. The results showed that the intracellular accumulation of DOX was much higher (17.1-6.6 fold increase) for glycomicelles as compared to that for LBA-free micelles (Fig. 4a). More interestingly, with an increase of LBA-functionality on the micelle surface, a higher intensity of DOX fluorescence was observed in the HepG2 cells. This is in line with a faster uptake rate of glycomicelles with a higher LBA density by the cells and also a more rapid release of DOX from glycomicelles with a higher LBA content. For example, the cellular concentration of free DOX was more than 2 times higher for GP80-PCL micelles than that for GP40-PCL micelles (Fig. 4b), although the release rate of DOX from these micelles in medium at pH 7.4 was not very much different. However, there was no obvious difference between the cellular concentration of DOX for GP80-PCL micelles and GP100-PCL micelles (Fig. 4b), which indicated that receptor-mediated endocytosis could not be improved any more beyond a certain level of sugar-ligands present in the micelles.¹⁹ These findings further demonstrate the high affinity of glycomicelles for HepG2 cells.

Anti-tumor activity of DOX-loaded micelles

The targeted anti-tumor activity of DOX-loaded glycomicelles was tested by the MTT assay using HepG2 cells. The cells were incubated with glycomicelles loaded with varying DOX dosages for 72 h. As expected, the cell deaths caused by the DOX-loaded glycomicelles were much higher than that of DOX-loaded non-glycomicelles (Fig. 5a). For example, the IC₅₀ values for GP100-PCL, GP80-PCL, GP40-PCL, GP20-PCL, and P(EO)-PCL micelles were estimated to be 0.43, 0.45, 0.75, 2.05 and 6.55 μg DOX equiv./mL, respectively. It should be noted that the viability of HepG2 cells was more efficiently suppressed with glycomicelles

with a higher LBA content at the same DOX concentration. Zhang *et al.* also demonstrated that oridonin-loaded chitosan-based nanogels with higher degrees of galactose-decoration from 2.44 to 14.04% presented better antitumor activity against HepG2 cells and are much more effective than drug-loaded nanogels without galactosylation.⁴⁴ We also found that when the LBA content reached 80%, the anti-tumor activity of DOX-loaded glycomicelles could not be improved any more by increasing the LBA density on the micelle surface, which is in line with the observation of targeted cellular uptake of DOX-loaded glycomicelles. The toxicity of DOX-loaded glycomicelles with high LBA-density was somewhat lower than that of free DOX ($IC_{50} = 0.20 \mu\text{g/mL}$), which could be possibly attributed to the attenuated DOX release from the LBA-decorated micelles. Moreover, glycomicelles with different LBA contents caused similar cytotoxic effects (ca. $5.0 \mu\text{g DOX equiv./mL}$ of IC_{50} values) to MCF-7 cells (low ASGP-R expression, negative control) under otherwise identical conditions (Fig. 5b). Importantly, MTT assays revealed that micelles were non-toxic to HepG2 and MCF-7 cells with cell viabilities of more than 92% up to a tested concentration of 0.50 mg/mL (Fig. 6). More interestingly, HepG2 cells were first incubated for 4 h with glycomicelles at a DOX dosage of $5 \mu\text{g/mL}$; media were aspirated and replenished with fresh culture media, and cells were further cultured for another 72 h. The cellular uptake of DOX-loaded glycomicelles can take place efficiently by HepG2 cells via receptor-mediated endocytosis. The result showed that glycomicelles with higher LBA densities progressively induced higher levels of HepG2 cell death. For instance, the cell viabilities of free HepG2 cells (- LBA) incubated with DOX-loaded GP100-PCL, GP80-PCL, GP40-PCL, and GP20-PCL micelles were 38.2, 29.2, 53.4 and 65.2%, respectively (Fig. 7), which were lower than the cell viability for DOX loaded LBA-free micelles (86.3%). The anti-tumor activity of DOX-loaded glycomicelles was reduced by pre-treating HepG2 cells with LBA, and the different LBA densities on DOX-loaded glycomicelles had little influence on the cell death

(ca. 80% cell viability). These results prove that DOX-loaded glycomicelles possess apparent targetability to HepG2 cells, and can efficiently provoke specific cell death, and the anti-tumor activity can be largely improved by increasing the LBA density on the glycomicelles.

Conclusion

We have demonstrated the successful synthesis of amphiphilic biodegradable glycopolymers with controlled LBA-functionality, which can be self-assembled into glycomicelles with different LBA-ligand densities on the surface. The glycomicelles present excellent cellular uptake by ASGP-R positive HepG2 liver cancer cells, resulting in significant in vitro antitumor activity. More interestingly, increasing the LBA-ligand density on the glycomicellar surface can improve the rate of micelle uptake by HepG2 cells as well as the accumulation of DOX in the cells. Hence, a higher LBA density on DOX-loaded glycomicelles can induce superior anti-tumor activity towards HepG2 cells. However, considering the balance of the tumor-targeting ligand surface density and the anti-biofouling surface properties, further in vivo experiments using a liver tumor model are being carried out in our lab. In principle, the remaining AC units after LBA and oligo(EO) modification can be used for crosslinking to further improve the stability of the micelles. We are convinced that these biodegradable glycomicelles with tailored LBA-ligand density can provide an interesting platform for designing delivery vehicles that target cancer cells contributing to the development of nano-scale diagnostic and therapeutic modalities.

Acknowledgements

This work was supported by the National Natural Science Foundation of China (NSFC 51003070, 51103093, 51173126, and 51273139), the National Science Fund for Distinguished Young Scholars (51225302), and a Project Funded by the Priority Academic Program Development of Jiangsu Higher Education Institutions.

References

1. L. S. Nair and C. T. Laurencin, *Prog. Polym. Sci.*, 2007, **32**, 762.
2. N. Wiradharma, Y. Zhang, S. Venkataraman, J. L. Hedrick and Y. Y. Yang, *Nano Today*, 2009, **4**, 302.
3. D. J. A. Cameron and M. P. Shaver, *Chem. Soc. Rev.*, 2011, **40**, 1761.
4. C. Deng, Y. Jiang, R. Cheng, F. Meng and Z. Zhong, *Nano Today*, 2012, **7**, 467.
5. J. Nicolas, S. Mura, D. Brambilla, N. Mackiewicz and P. Couvreur, *Chem. Soc. Rev.*, 2013, **42**, 1147.
6. M. E. Davis, Z. Chen and D. M. Shin, *Nat. Rev. Drug Discov.*, 2008, **7**, 771.
7. M. Yokoyama, *Expert Opin. Drug Deliv.*, 2010, **7**, 145.
8. K. Kataoka, A. Harada and Y. Nagasaki, *Adv. Drug Deliv. Rev.*, 2012, **64**, 37.
9. G. Pasut and F. M. Veronese, *Adv. Drug Deliv. Rev.*, 2009, **61**, 1177.
10. K. Knop, R. Hoogenboom, D. Fischer and U. S. Schubert, *Angew. Chem. Int. Ed.*, 2010, **49**, 6288.
11. F. Danhier, O. Feron and V. Préat, *J. Control. Release*, 2010, **148**, 135.
12. H. Koo, M. S. Huh, I.-C. Sun, S. H. Yuk, K. Choi, K. Kim and I. C. Kwon, *Acc. Chem. Res.*, 2011, **44**, 1018.
13. J. H. Ryu, H. Koo, I.-C. Sun, S. H. Yuk, K. Choi, K. Kim and I. C. Kwon, *Adv. Drug Deliv. Rev.*, 2012, **64**, 1447.
14. Y. Zhong, F. Meng, C. Deng and Z. Zhong, *Biomacromolecules*, 2014, **15**, 1955.
15. T. M. Allen, *Nat. Rev. Cancer*, 2002, **2**, 750.
16. M. Elsabahy and K. L. Wooley, *Chem. Soc. Rev.*, 2012, **41**, 2545.
17. Y. C. Lee and R. T. Lee, *Acc. Chem. Res.*, 1995, **28**, 321.
18. A. Martinez, C. Ortiz Mellet and J. M. Garcia Fernandez, *Chem. Soc. Rev.*, 2013, **42**, 4746.

19. F. Gu, L. Zhang, B. A. Teply, N. Mann, A. Wang, A. F. Radovic-Moreno, R. Langer and O. C. Farokhzad, *Proc. Natl. Acad. Sci. USA*, 2008, **105**, 2586.
20. R. P. Brinas, A. Sundgren, P. Sahoo, S. Morey, K. Rittenhouse-Olson, G. E. Wilding, W. Deng and J. J. Barchi, Jr., *Bioconjugate Chem.*, 2012, **23**, 1513.
21. C. R. Becer, *Macromol. Rapid Commun.*, 2012, **33**, 742.
22. B. Lepenies, J. Lee and S. Sonkaria, *Adv. Drug Deliv. Rev.*, 2013, **65**, 1271.
23. C. R. Bertozzi and a. L. L. Kiessling, *Science*, 2001, **291**, 2357.
24. A. Top and K. L. Kiick, *Adv. Drug Deliv. Rev.*, 2010, **62**, 1530.
25. D. J. Siegwart, J. K. Oh and K. Matyjaszewski, *Prog. Polym. Sci.*, 2012, **37**, 18.
26. J. J. Lundquist and E. J. Toone, *Chem. Rev.*, 2002, **102**, 555.
27. Z. Deng, S. Li, X. Jiang and R. Narain, *Macromolecules*, 2009, **42**, 6393.
28. S. K. Mamidyala, S. Dutta, B. A. Chrnyk, C. Prévaille, H. Wang, J. M. Withka, A. McColl, T. A. Subashi, S. J. Hawrylik, M. C. Griffor, S. Kim, J. A. Pfefferkorn, D. A. Price, E. Menhaji-Klotz, V. Mascitti and M. G. Finn, *J. Am. Chem. Soc.*, 2012, **134**, 1978.
29. P. a. Ma, S. Liu, Y. Huang, X. Chen, L. Zhang and X. Jing, *Biomaterials*, 2010, **31**, 2646.
30. S. Alonso, M. Rendueles and M. Díaz, *Biotechnol. Adv.*, 2013, **31**, 1275.
31. Y. Zhong, W. Yang, H. Sun, R. Cheng, F. Meng, C. Deng and Z. Zhong, *Biomacromolecules*, 2013, **14**, 3723.
32. A. E. Smith, A. Sizovs, G. Grandinetti, L. Xue and T. M. Reineke, *Biomacromolecules*, 2011, **12**, 3015.
33. J. Kumar, A. Bousquet and M. H. Stenzel, *Macromol. Rapid Commun.*, 2011, **32**, 1620.
34. Y. Wang, X. Zhang, P. Yu and C. Li, *Int. J. Pharm.*, 2013, **441**, 170.
35. J. Ding, C. Xiao, Y. Li, Y. Cheng, N. Wang, C. He, X. Zhuang, X. Zhu and X. Chen, *J. Control. Release*, 2013, **169**, 193.
36. Y. Wang, C.-Y. Hong and C.-Y. Pan, *Biomacromolecules*, 2013, **14**, 1444.
37. Y. Tao, J. He, M. Zhang, Y. Hao, J. Liu and P. Ni, *polym. Chem.*, 2014, **5**, 3443.
38. H. M. Branderhorst, R. M. J. Liskamp, G. M. Visser and R. J. Pieters, *Chem. Commun.*, 2007, **0**, 5043.
39. L. Sun, Y. Yang, C.-M. Dong and Y. Wei, *Small*, 2011, **7**, 401.
40. V. Percec, P. Leowanawat, H.-J. Sun, O. Kulikov, C. D. Nusbaum, T. M. Tran, A. Bertin, D. A. Wilson, M. Peterca, S. Zhang, N. P. Kamat, K. Vargo, D. Moock, E. D. Johnston, D. A. Hammer, D. J. Pochan, Y. Chen, Y. M. Chabre, T. C. Shiao, M. Bergeron-Brlek, S.

- André, R. Roy, H.-J. Gabius and P. A. Heiney, *J. Am. Chem. Soc.*, 2013, **135**, 9055.
41. S. Pearson, W. Scarano and M. H. Stenzel, *Chem. Commun.*, 2012, **48**, 4695.
42. R. Ma, H. Yang, Z. Li, G. Liu, X. Sun, X. Liu, Y. An and L. Shi, *Biomacromolecules*, 2012, **13**, 3409.
43. L. X. Yang, H. H. Xiao, L. S. Yan, R. Wang, Y. B. Huang, Z. G. Xie and X. B. Jing, *J. Mater. Chem. B*, 2014, **2**, 2097.
44. C. Duan, J. Gao, D. Zhang, L. Jia, Y. Liu, D. Zheng, G. Liu, X. Tian, F. Wang and Q. Zhang, *Biomacromolecules*, 2011, **12**, 4335.
45. F. Suriano, R. Pratt, J. P. K. Tan, N. Wiradharma, A. Nelson, Y.-Y. Yang, P. Dubois and J. L. Hedrick, *Biomaterials*, 2010, **31**, 2637.
46. W. Chen, Y. Zou, F. Meng, R. Cheng, C. Deng, J. Feijen and Z. Zhong, *Biomacromolecules*, 2014, **15**, 900.
47. W. Chen, H. Yang, R. Wang, R. Cheng, F. Meng, W. Wei and Z. Zhong, *Macromolecules*, 2010, **43**, 201.
48. W. Chen, F. Meng, R. Cheng, C. Deng, J. Feijen and Z. Zhong, *J. Control. Release*, 2014, **190**, 398.
49. H.-b. Xie, L. Jin, S. Rudić, J. P. Simons and R. B. Gerber, *J. Phys. Chem. B*, 2012, **116**, 4851.
50. F. Kohori, M. Yokoyama, K. Sakai and T. Okano, *J. Control. Release*, 2002, **78**, 155.
51. X. Shuai, H. Ai, N. Nasongkla, S. Kim and J. Gao, *J. Control. Release*, 2004, **98**, 415.
52. R. Cheng, X. Wang, W. Chen, F. Meng, C. Deng, H. Liu and Z. Zhong, *J. Mater. Chem.*, 2012, **22**, 11730.
53. Y. Li, Z.-Y. Tang and J.-X. Hou, *Nat. Rev. Gastroenterol. Hepatol.*, 2012, **9**, 32.
54. Y. Zou, Y. Song, W. Yang, F. Meng, H. Liu and Z. Zhong, *J. Control. Release*, 2014, **193**, 154.
55. R. Yang, F. Meng, S. Ma, F. Huang, H. Liu and Z. Zhong, *Biomacromolecules*, 2011, **12**, 3047.

Table 1 Characteristics of biodegradable glycopolymer-PCL micelles with tailored LBA-functionality.

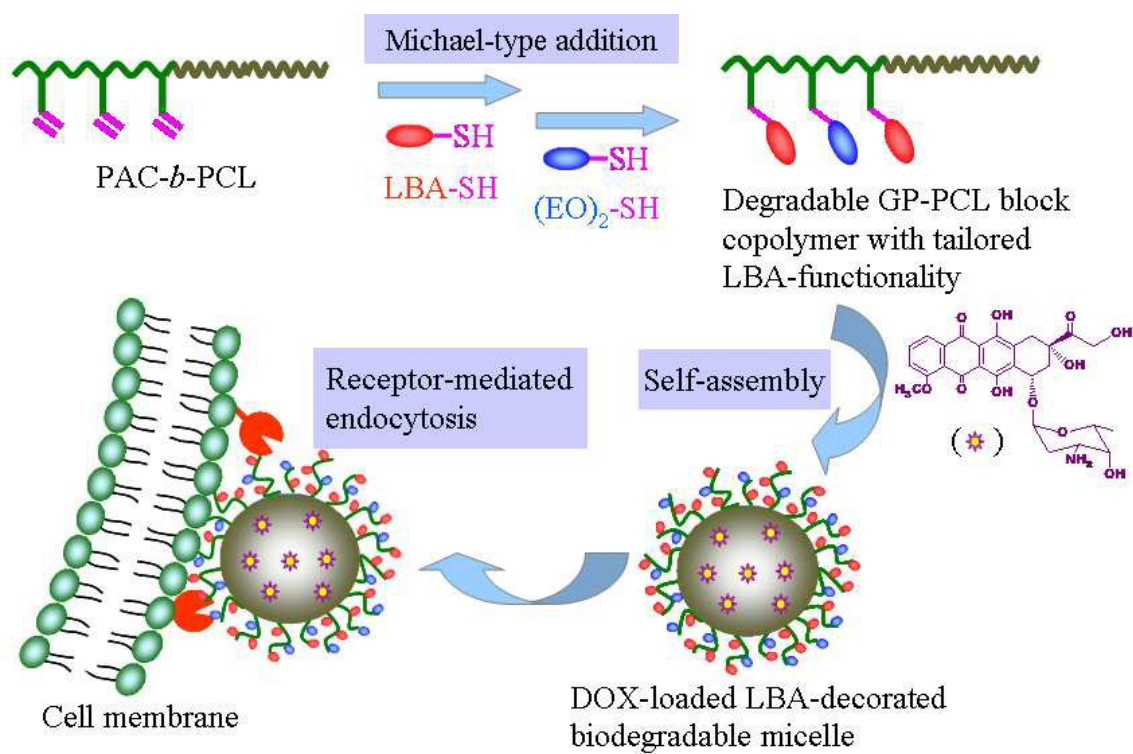
Entry	Functional copolymer ^a	Size (nm) ^b	PDI ^b	ζ (mV) ^b	CMC (mg/L) ^c
1	GP100-PCL	31.9 ± 1.6	0.18	5.3 ± 1.2	3.72
2	GP80-PCL	38.5 ± 2.3	0.12	-0.1 ± 1.7	1.87
3	GP40-PCL	57.3 ± 1.5	0.13	-3.2 ± 0.8	1.43
4	GP20-PCL	76.8 ± 1.2	0.10	-8.2 ± 1.4	1.35
5	P(EO)-PCL	88.2 ± 0.9	0.07	-16.5 ± 2.4	1.03

^a Synthesized by sequential post-polymerization modification of PAC-*b*-PCL block copolymer by Michael-type addition reaction with LBA-SH and/or (EO)₂-SH; ^b The average particle size (nm), size distribution and ζ -potentials measured by DLS at a micelle concentration of 0.2 mg/mL in water; ^c Critical micelle concentration determined using pyrene as a fluorescent probe.

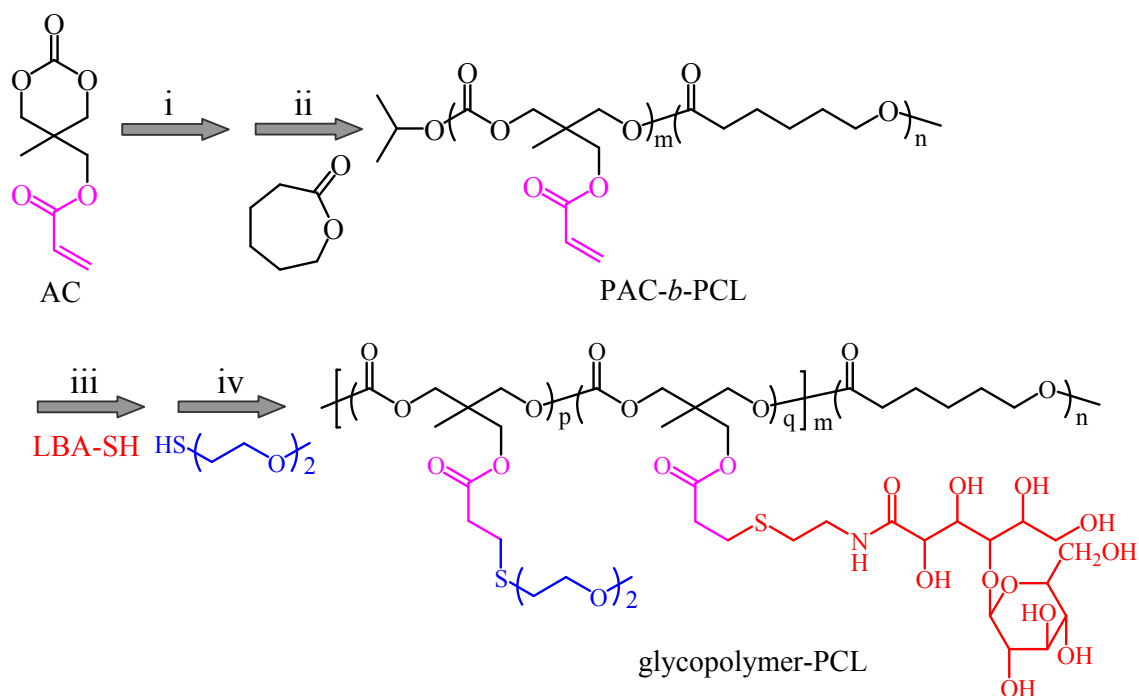
Table 2 Characteristics of DOX-loaded biodegradable glycopolymer-PCL micelles with different amounts of LBA at a theoretical DLC of 20 wt.%.

Entry	Micelle	DLC (wt.%) ^a	DLE (%)	Size (nm) ^b	PDI ^b
1	GP100-PCL	17.8	89.2	42.6 ± 2.1	0.20
2	GP80-PCL	17.1	85.5	50.3 ± 1.8	0.17
3	GP40-PCL	16.8	86.2	61.2 ± 2.6	0.15
4	GP20-PCL	16.6	83.0	75.1 ± 1.4	0.17
5	P(EO)-PCL	16.5	82.3	81.5 ± 1.7	0.16

^a DOX loading content determined by fluorescence measurements; ^b Determined by DLS.



Scheme 1 Illustration of versatile construction of biodegradable glycopolymer-PCL micelles with tailored LBA-functionality for hepatoma-targeted drug delivery.



Scheme 2 Synthesis of amphiphilic block glycopolymer by one-pot sequential ring-opening polymerization of AC and ϵ -CL in DCM using isopropanol as an initiator and zinc bis[bis(trimethylsilyl)amide] as a catalyst, followed by sequential post-polymerization modification with thiolated molecules through Michael-type conjugate addition reaction. Conditions: (i) r.t., 4 h; (ii) 40 °C, 20 h; (iii) r.t., 8 h; (iv) r.t. 8 h.

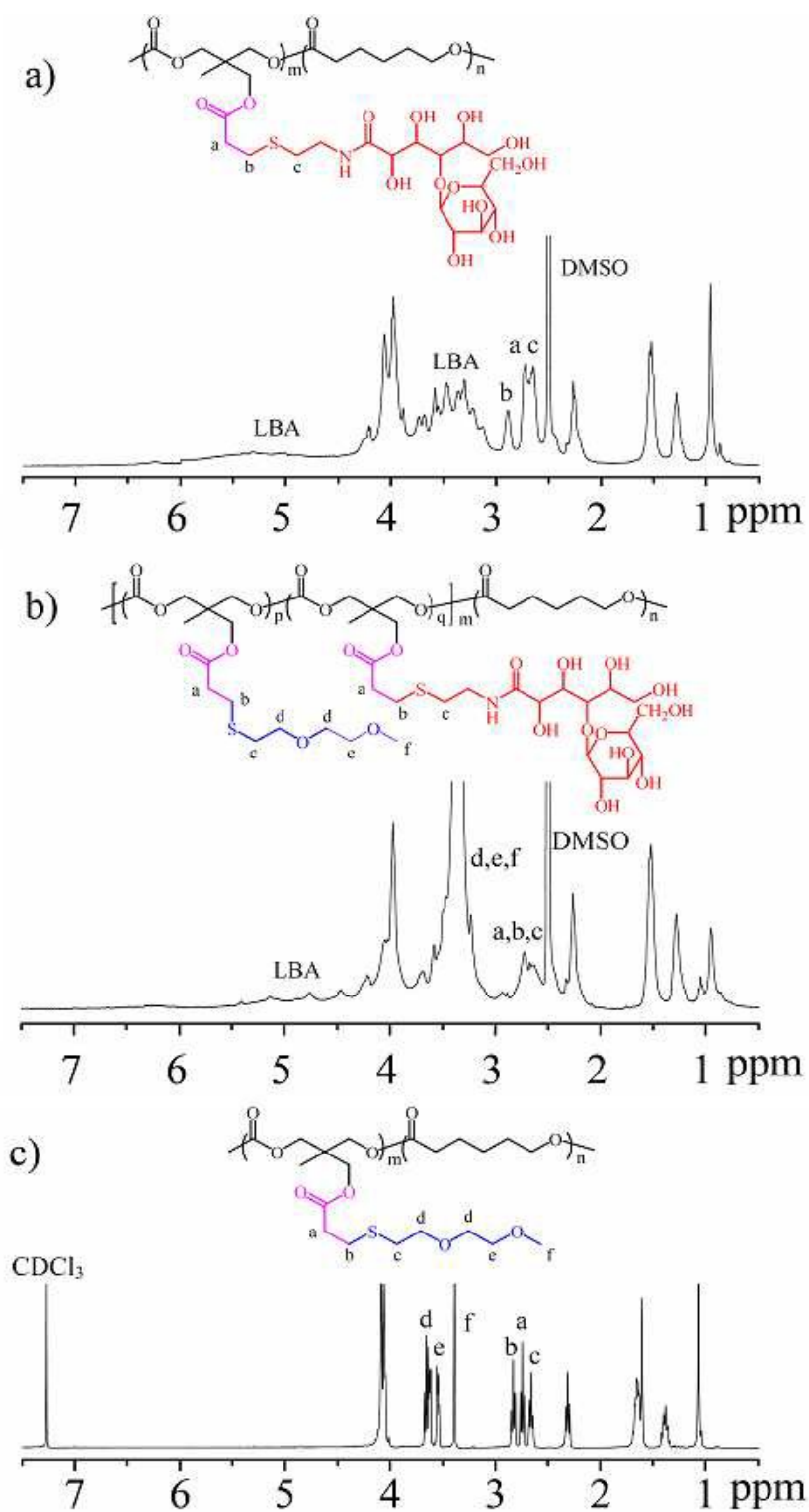


Fig.1 ^1H NMR spectra (400 MHz) of PAC-*b*-PCL copolymer modified with LBA-SH and (EO)₂-SH. (a) GP100-PCL; (b) GP40-PCL; (c) P(EO)-PCL.

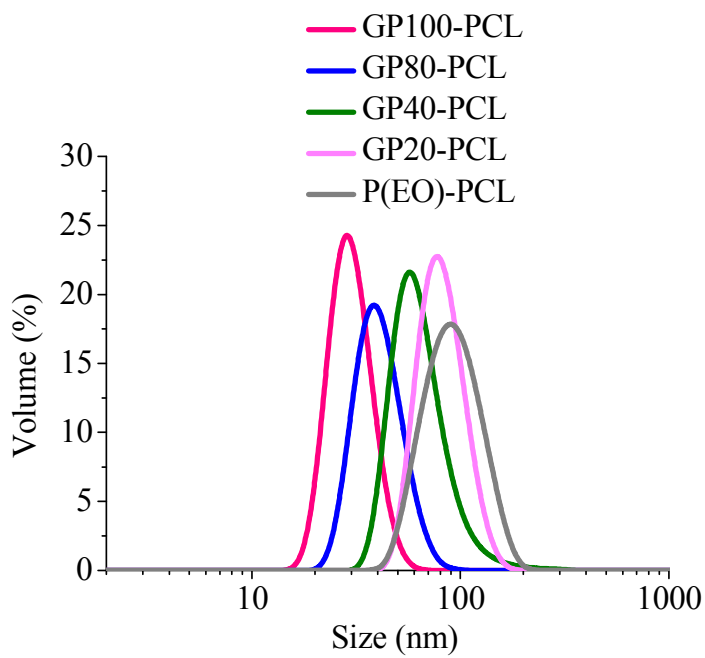


Fig. 2 Size distribution of biodegradable glycopolymer-PCL micelles with different contents of LBA determined by DLS.

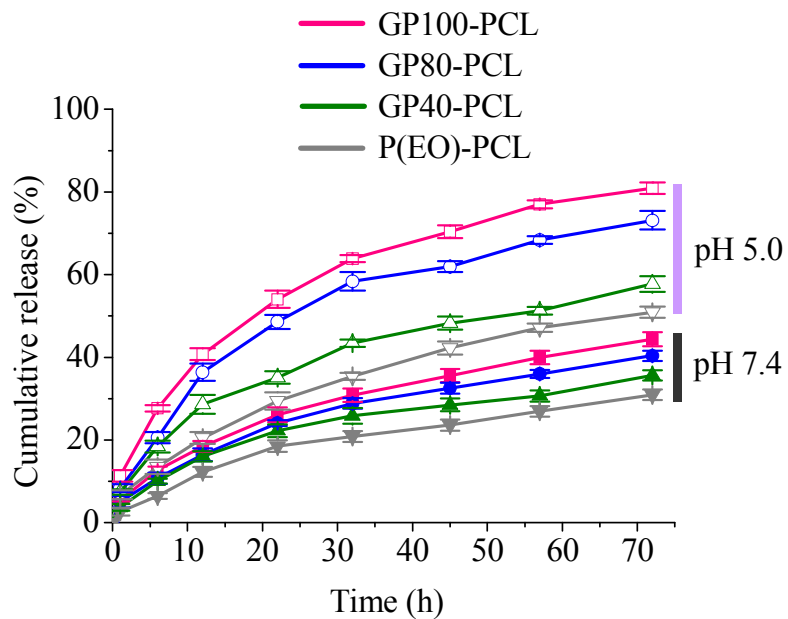


Fig. 3 *In vitro* release profiles of DOX from DOX-loaded glycopolymer-PCL micelles in PB (10 mM, pH 7.4) or acetate buffer (10 mM, pH 5.0) at 37 °C.

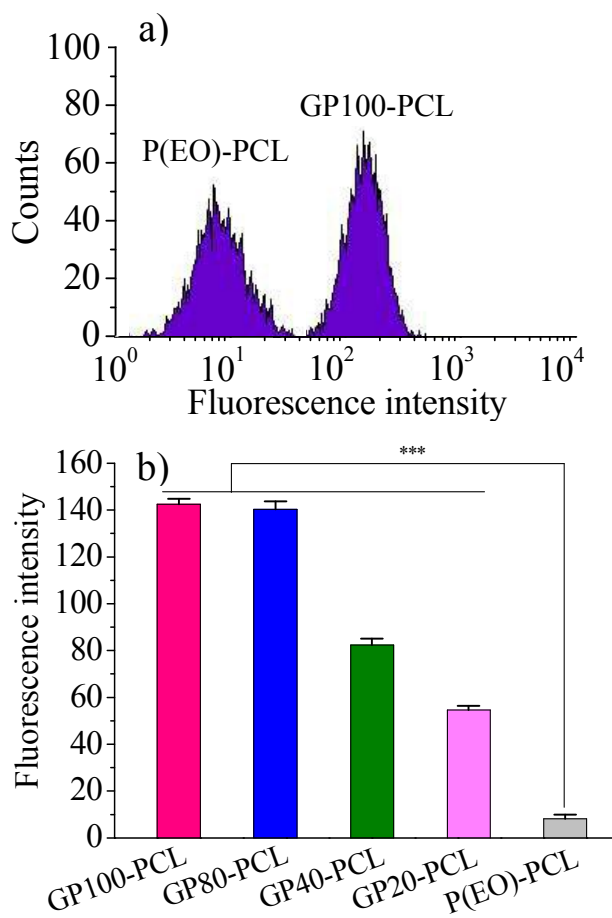


Fig. 4 Flow cytometric analysis of HepG2 cells after 4h incubation with DOX-loaded glycopolymer-PCL micelles or non-glycomicelles (DOX concentration of 5 $\mu\text{g}/\text{mL}$; cell counts 10000). (a) Histogram of HepG2 cells after incubation with DOX-loaded GP100-PCL or P(EO)-PCL micelles, respectively; (b) Maximal fluorescence intensities of HepG2 cells after incubation with different DOX-loaded glycomicelles and non-glycomicelles (Student's t test, *** $p < 0.001$).

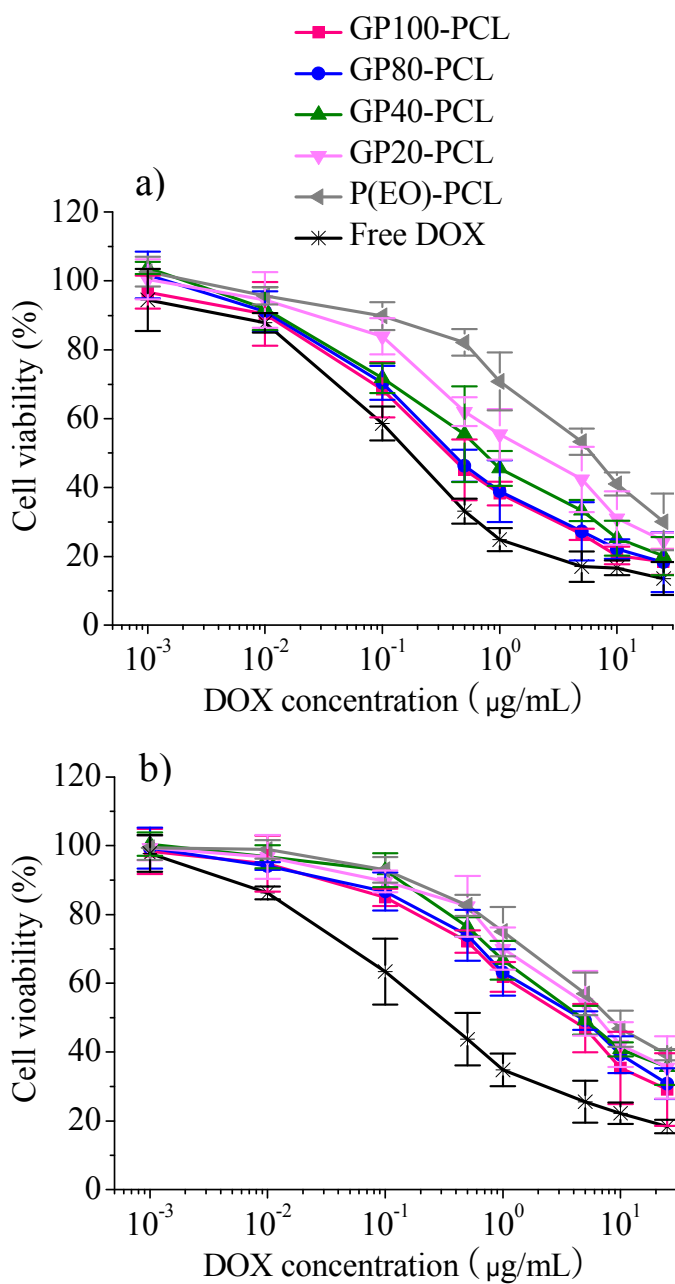


Fig. 5 Viabilities of HepG2 cells (a) and MCF-7 cells (b) following 72 h incubation with DOX-loaded glycopolymer-PCL micelles and free DOX as a function of DOX concentration. The data are presented as the average \pm standard deviation ($n = 4$).

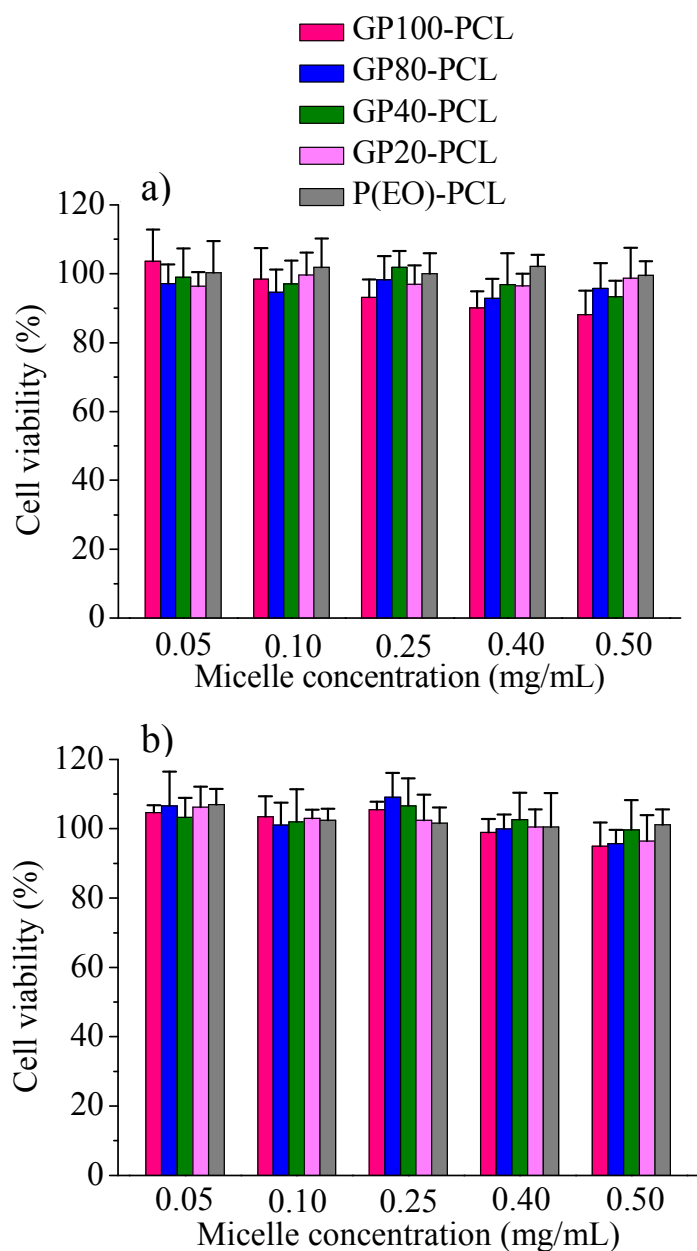


Fig. 6 Cytotoxicity of glycopolymer-PCL micelles using HepG2 cells (a) and MCF-7 cells (b).

The cells were incubated with micelles for 72 h. Data are presented as the average \pm standard deviation ($n = 4$).

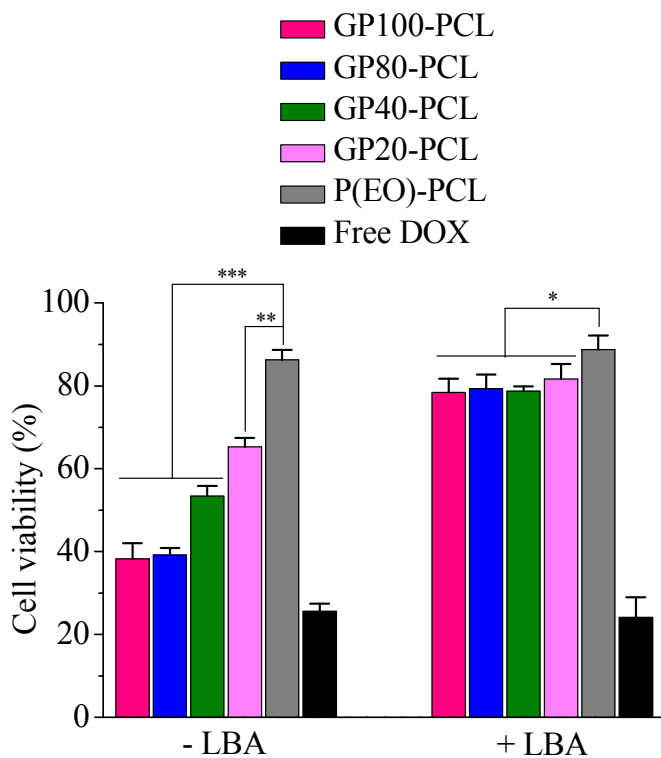


Fig. 7 Cytotoxicity of DOX-loaded micelles by MTT assay using HepG2 cells. The cells were incubated with free LBA (+ LBA) or without free LBA (- LBA) for 4 h, then the medium was replaced by 90 μL of fresh DMEM medium and 10 μL of DOX-loaded micelles or free DOX. DOX dosage was 10 $\mu\text{g}/\text{mL}$. After 4 h incubation, the medium was replaced by 100 μL of fresh DMEM medium and the cells were cultured for another 72 h. Data are presented as the average \pm standard deviation ($n = 4$, Student's t test, * $p < 0.05$, ** $p < 0.01$, *** $p < 0.001$).

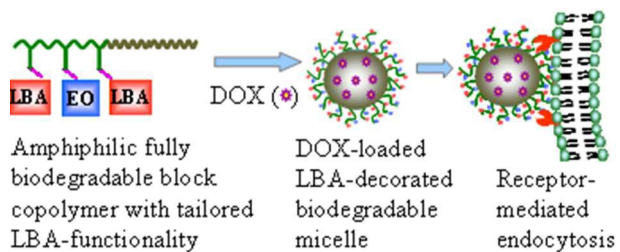
Table of Content:

Illustration of versatile construction of biodegradable glycopolymer-PCL micelles with tailored LBA-functionality for hepatoma-targeted drug delivery.